Available online at www.sciencedirect.com
ScienceDirect
Journal of Crystal Growth 301–302 (2007) 735–739
JOURNAL OF CRYSTAL GROWTH
www.elsevier.com/locate/jcrysgro

Self-assembled lateral Bi-quantum-dot molecule formation by gas-source molecular beam epitaxy

S. Suraprapapich[a,b,*], Y.M. Shen[a], V.A. Odnoblyudov[a], Y. Fainman[a], S. Panyakeow[b], C.W. Tu[a]

[a]*Department of Electrical and Computer Engineering, University of California San Diego, La Jolla, CA 92093-0407, USA*
[b]*Department of Electrical Engineering, Chulalongkorn University, Bangkok 10330, Thailand*

Available online 9 January 2007

Abstract

Self-assembled InAs bi-quantum-dot molecules (BQDMs) on GaAs (0 0 1) have been achieved using gas-source molecular beam epitaxy (GSMBE) and characterized by atomic force microscopy (AFM) and photoluminescence (PL) measurements. After the initial InAs quantum dots are partially capped with GaAs and followed by deposition of InAs, BQDMs are formed. Photoluminescence spectra of BQDMs can be described by two Gaussian-fitted curves at low temperature due to two different dot sizes. This is consistent with dot height histograms obtained from AFM images of BQDMs. For PL intensity, thermal quenching is observed at temperatures above 100 K. The activation energy of BQDM PL corresponds to nonradiative recombination due to defected-related states and potential fluctuation.

Keywords: A1. Bi-quantum-dot molecule; A3. Gas-source molecular beam epitaxy

1. Introduction

Self-assembled semiconductor quantum dots (QDs), from highly strained-layer heteroepitaxy in the Stranski–Krastanow (S–K) growth mode, have been intensively studied because of the δ-function-like density of states [1–3], which is significant for optoelectronic applications [4–6]. Spontaneous formation of semiconductor quantum-dot molecules (QDMs), which are clusters of QDs, has attracted attention as a possible implementation of future quantum devices such as quantum cellular automata [7,8]. Lateral QDMs have been achieved by several growth techniques, such as a combination of in situ etching and self-assembly [9] and self-assembly by anisotropic strain engineering on an In(Ga)As/GaAs (311B) superlattice (SL) template [10]. In our previous work, lateral QDMs have also been obtained using a thin-capping-and-regrowth technique by solid-source molecular beam epitaxy (SSMBE) under As_4 overpressure [11]. After isolated self-assembled QDs are capped partially with GaAs, nanoholes (camel-like nanostructure) are formed. The nanoholes are controlled by varying the capping temperature. InAs is then deposited (regrowth), and QDMs are formed at 430 °C with at least five dots per QDM [12].

In this paper, the formation of InAs bi-quantum-dot molecules (BQDMs) is achieved on a GaAs substrate by gas-source MBE (GSMBE) under As_2 overpressure using the thin-capping-and-regrowth technique. Morphological studies by atomic force microscopy (AFM) and temperature dependence of BQDM optical properties are investigated. A comparison of quantum structures grown under different arsenic species (dimers and tetramers) is underway and will be presented elsewhere.

2. Experimental procedure

All samples are grown on (0 0 1) semi-insulating GaAs substrates by GSMBE in a modified Varian Gen-II system. Elemental Ga and In are used as the group-III sources, and thermally cracked arsine, which produces As_2 and H_2, is

*Corresponding author. Department of Electrical Engineering, Chulalongkorn University, Bangkok 10330, Thailand.
E-mail addresses: suwaree.s@student.chula.ac.th (S. Suraprapapich), s_panyakeow@yahoo.com (S. Panyakeow).

0022-0248/$ - see front matter © 2006 Elsevier B.V. All rights reserved.
doi:10.1016/j.jcrysgro.2006.11.120

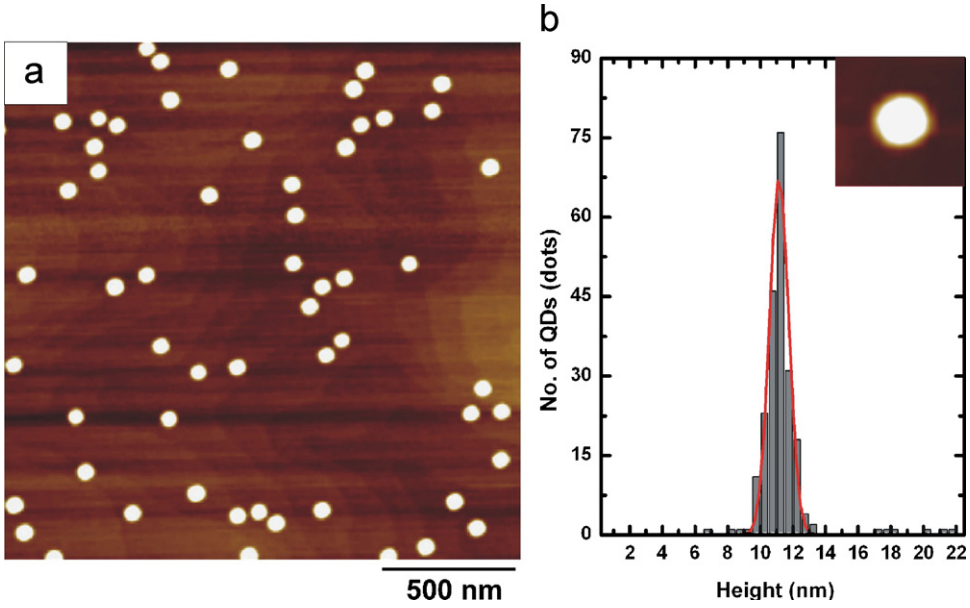

Fig. 1. AFM image (a) and dot height histogram with Gaussian fit (b) of as-grown QDs.

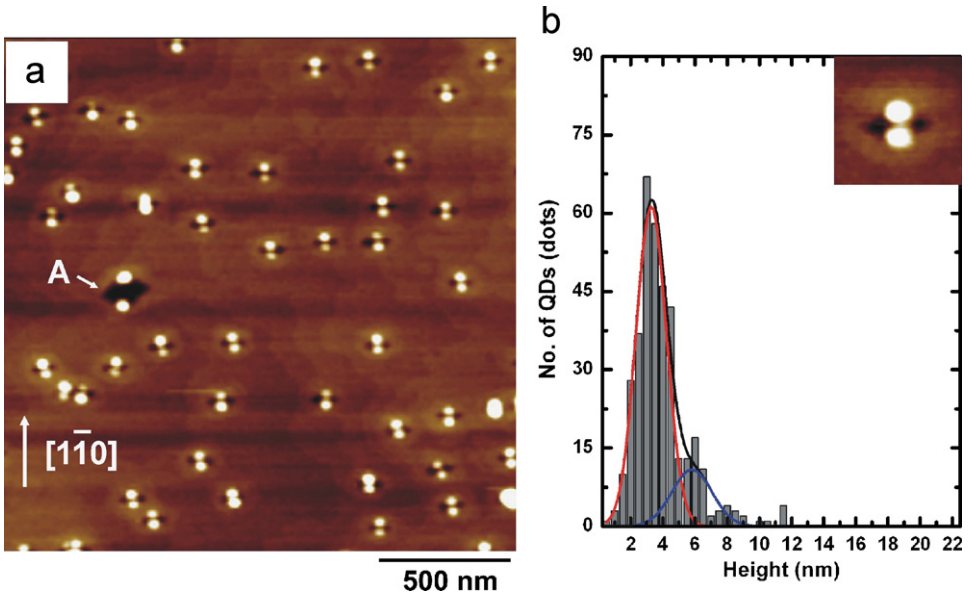

Fig. 2. AFM image (a) and dot height histogram with Gaussian fit (b) of BQDMs.

used as the group-V source. The growth rates of GaAs and InAs are 0.6 monolayer (ML) per second and 0.01 ML/s, respectively. After oxide desorption, a 300-nm-thick GaAs buffer layer is grown at a temperature of 580 °C. Under As_2 overpressure and deposition of 1.8 ML amount of InAs, QDs are formed randomly on the surface at a temperature of 500 °C. Then, the substrate temperature is ramped down to 470 °C and InAs QDs are capped partially with a 6-ML-thick GaAs layer. When 0.6-ML-thick InAs is deposited, BQDMs are formed on the partially covered InAs QDs. Then a 150-nm thick GaAs buffer layer is grown and the thin-capping-and-regrowth process is repeated once more. The dot formation is monitored in situ by reflection high-energy-electron diffraction (RHEED). After growth the sample is ramped down immediately to room temperature. The embedded BQDMs are for PL measurements, and the top BQDMs for AFM measurements. A separate sample is grown with only QDs as a reference ("as-grown QDs").

Surface morphology is imaged by tapping-mode AFM with a sharpened SiN tip on uncapped samples. PL measurements are carried out in a close-cycle He cryostat at various temperatures and excitation power densities. A diode-pumped solid-state laser at 532 nm emission wavelength is used for excitation and the signal is dispersed in a 0.5 m monochromator and detected by a thermoelectrically cooled InGaAs photodiode using standard lock-in technique.

3. Results and discussion

Figs. 1(a) and 2(a) show AFM image of as-grown QDs at a coverage of 1.8 ML and BQDMs, respectively. BQDMs are oriented along the [1 $\bar{1}$ 0] crystallographic direction. The dot density of as-grown QDs is $6 \times 10^9\,cm^{-2}$, whereas the total QD density in the BQDM sample is $1.1 \times 10^{10}\,cm^{-2}$, consisting of 9.4×10^9 QDs cm^{-2} from 4.7×10^9 BQDMs cm^{-2}, and 1.9×10^9 QDs cm^{-2}. Each as-grown QD is transformed into a BQDM after the thin-capping-and-regrowth procedure, but the BQDM density is lower due to merging of some BQDMs into single dots. Figs. 1(b) and 2(b) show dot height histograms obtained from AFM images of as-grown QDs and BQDMs, respectively. Note that the QDs in the BQDM sample are largely comprised of smaller dots than as-grown QDs. The histogram in Fig. 3 shows the center-to-center separation of BQDMs, and it is fitted with a Gaussian distribution with an average separation of 22 nm. This relatively large separation shows that the PL observed from BQDMs, shown below, is from individual QDs in the BQDMs.

Fig. 4 shows PL spectra of as-grown QDs and BQDMs at 9 K with excitation power density ranging from 0.13 to 8 kW/cm^2. The highest peaks of as-grown QDs and BQDMs spectra are at 1.08 and 1.195 eV with full-width at-half maximum (FWHM) of 28 and 60 meV, respectively. The spectrum of the BQDMs can be described by two Gaussian curves composed of a higher peak at 1.19 eV and a smaller peak at 1.128 eV. These results confirm the bimodal distribution of dot heights. The PL spectra are normalized to the highest peak. As the incident excitation power increases, the higher energy peak of the as-grown QD sample increases relative to the lower-energy peak. This indicates that the lower-energy peak is from ground-state transitions and saturated, and the higher energy peak is from transitions between the first excited states. On the other hand, the relative intensity of the two peaks in BQDMs PL remains the same with increasing incident excitation power, indicating these two peaks are from ground-state transition from QDs with different dot sizes, as shown in Fig. 2(b).

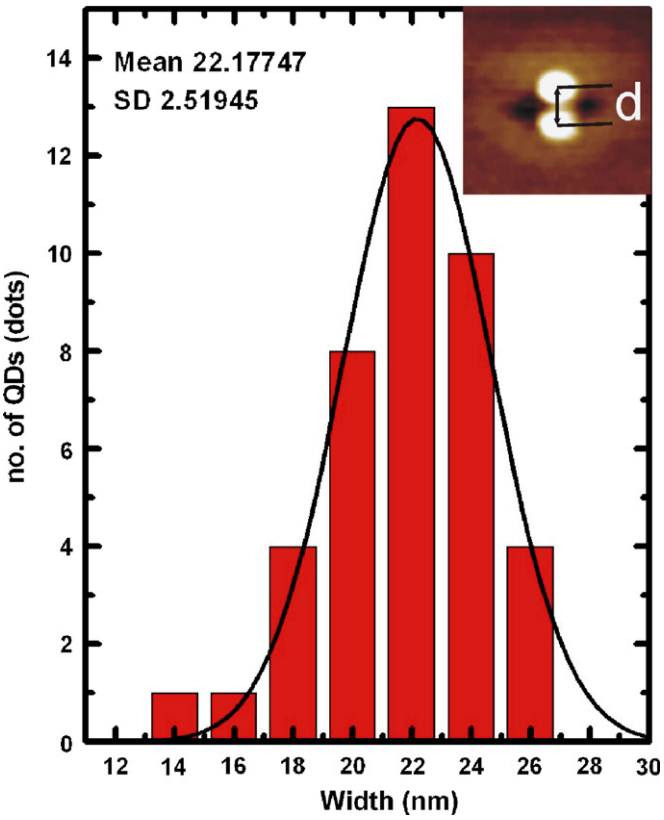

Fig. 3. Center-to-center width histogram of BQDMs with Gaussian fit.

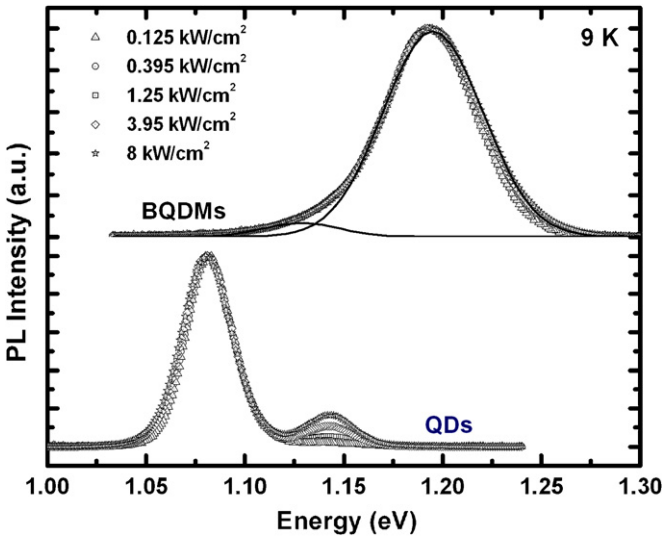

Fig. 4. PL spectra of as-grown QDs and BQDMs at 9 K. The dotted curves for BQDMS are the Gaussian components.

Despite higher dot density, the PL intensity of BQDMs is lower than that of QDs. It is attributed to defects such as nanovoids, as shown by "A" in Fig. 2(a), which could affect the optical efficiency due to nonradiative recombination.

Temperature-dependent PL data from 9 to 290 K are also obtained while the incident excitation intensity is held constant at 10 kW/cm^2. Fig. 5 shows the temperature dependence of the peak emission energy, which can be fitted by the Varshni model [13]

$$E(T) = E_0 - \frac{\alpha T^2}{T + \beta}, \tag{1}$$

where $E(T)$ and E_0 are the peak energies at T and 0 K, respectively, and α and β are constants. The variation of the peak emission energy with temperature can be attributed to the effect of dilation of lattice and electron–lattice interaction. The solid line in Fig. 5 is the Varshni equation with $E_0 = 1.083$ eV for as-grown QDs and 1.198 eV for BQDMs, $\alpha = 3.16 \times 10^{-4}$ eV/K and $\beta = 93$ K for both as-grown QDs and BQDMs. The α and β values agree with those of InAs [13]. The maximum red shift of 23 meV in the BQDM curve from the Varshni equation is

probably due to transfer from smaller dot family (higher energy) to larger dot family (lower energy) within the QDs of the BQDM family, but not to the much larger dots in Fig. 4, where the energy difference is much larger, ~80 meV [14,15].

Fig. 6 shows the PL intensity of as-grown QDs and BQDMs vs. inverse temperature. As the measurement temperature increases from 9 K, the PL intensity of BQDMs remains constant up to 100 K and then rapidly quenches. The solid lines are fitted with an assumption of two thermally activated processes with [16,17].

$$I(T) = \frac{I(0)}{1 + Ae^{-E_a/kT} + Be^{-E_b/kT}}, \quad (2)$$

where $I(T)$ and $I(0)$ are the PL intensity at T and 0 K, respectively; A and B are constants; E_a and E_b are thermal activation energies. Activation energy E_a, derived from the slope of the straight-line portion (150–300 K) of the curves,

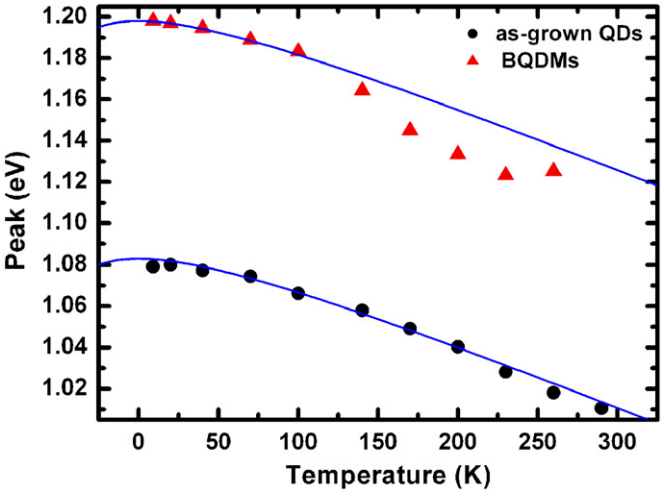

Fig. 5. The temperature-dependent peak emission energy of as-grown QDs and BQDMs. The solid lines are calculations from the Varshni equation.

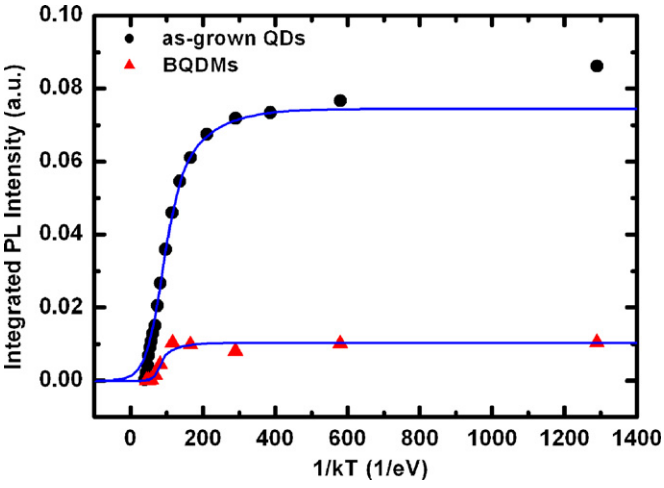

Fig. 6. The temperature dependence of PL intensity of as-grown QDs and BQDMs.

is 45 and 128 meV for as-grown QDs and BQDMs, respectively. The smaller energy E_b is ascribed to trapped excitons or carriers thermalizing from localized regions resulting from potential fluctuations due to size distribution of QDs. The larger energy of E_a corresponds to the difference in energy between the ground state and the wetting layer if there are no localized states. E_a for BQDMs then is expected to be smaller than E_a for as-grown QDs because of smaller dot size. Our results are contrary to this expectation, indicating the existence of non-radiative recombination centers in BQDMs between the QD energy level and the wetting layer energy level.

4. Conclusion

Self-assembled InAs lateral BQDMs have been achieved using GSMBE under As_2 overpressure. Gaussian distribution fits dot height histograms from AFM images. The temperature dependence of PL is investigated. The variation of the photon energy with temperature is tentatively attributed to size variation of QDs within the BQDMs. Temperature-dependent PL intensities indicate the existence of potential fluctuation due to QD size fluctuation and localized states in the wetting layer.

Acknowledgments

This work is partially supported by the Quantum Information Science and Technology (QuIST) program of the US Air Force Office of Scientific Research (AFOSR) and the Thailand Research Fund (TRF) through Royal Golden Jubilee and TRF's Senior Researcher Scholar, Asian Office of Aerospace Research and Development (AOARD) of the US Air Force, Chulalongkorn University and National Nanotechnology Center of Thailand.

References

[1] M. Sugawara, Self-Assembled InGaAs/GaAs Quantum Dots: Semiconductors and Semimetala, vol. 60, Academic Press, New York, 1999.
[2] W. Seifert, N. Carlsson, M. Miller, M.-E. Pistol, L. Samuelson, L.R. Wallenberg, Prog. Crystal Growth Charact. 33 (1996) 423.
[3] L.G. Wang, P. Kratzer, N. Moll, M. Scheffler, Phys. Rev. B 62 (2000) 1897.
[4] Y. Arakawa, H. Sakaki, Appl. Phys. Lett. 40 (1982) 939.
[5] M. Asada, Y. Miyamoto, Y. Suematsu, IEEE J. Quantum Electron. 22 (1986) 1915.
[6] S.-Y. Lin, Y.-J. Tsai, S.-C. Lee, Appl. Phys. Lett. 83 (2003) 752.
[7] C.S. Lent, P.D. Tougaw, W. Porod, Appl. Phys. Lett. 62 (1993) 714.
[8] J.R. Petta, A.C. Johnson, J.M. Taylor, E.A. Laird, A. Yacoby, M.D. Lukin, C.M. Marcus, M.P. Hanson, A.C. Gossard, Science 309 (2005) 2180.
[9] R. Songmuang, S. Kiravittaya, O.G. Schmidt, Appl. Phys. Lett. 82 (2003) 2892.
[10] T. van Lippen, R. Nötzel, G.J. Hamhuis, J.H. Wolter, Appl. Phys. Lett. 85 (2004) 118.
[11] S. Suraprapapich, S. Thainoi, S. Kanjanachuchai, S. Panyakeow, J. Vac. Sci. Technol. B 23 (2005) 1217.

[12] S. Suraprapapich, S. Thainoi, S. Kanjanachuchai, S. Panyakeow, Microelectron. Eng. 83 (2006) 1526.
[13] Y.P. Varshni, Physica 34 (1967) 149.
[14] A. Polimeni, A. Patanè, M. Henini, L. Eaves, P.C. Main, Phys. Rev. B 59 (1999) 5064.
[15] Z. Mi, P. Bhattacharya, J. Appl. Phys. 93 (2005) 023510.
[16] J.D. Lambkin, L. Considine, S. Walsh, G.M. O'Connor, C.J. McDonagh, T.J. Glynn, Appl. Phys Lett. 65 (1994) 73.
[17] A. Nishikawa, Y.G. Hong, C.W. Tu, J. Vac. Sci. Technol. B 22 (2004) 1515.